THE JOURNAL OF BIOLOGICAL CHEMISTRY
Vol. 279, No. 13, Issue of March 26, pp. 12860–12867, 2004

Printed in U.S.A.

Structural Studies on Flavin Reductase PheA2 Reveal Binding of NAD in an Unusual Folded Conformation and Support Novel Mechanism of Action*

Received for publication, December 16, 2003, and in revised form, December 23, 2003
Published, JBC Papers in Press, December 31, 2003, DOI 10.1074/jbc.M313765200

Robert H. H. van den Heuvel‡§¶, Adrie H. Westphal‖, Albert J. R. Heck§, Martin A. Walsh, Stefano Rovida‡, Willem J. H. van Berkel‖, and Andrea Mattevi‡ ‡‡**

*From the ‡Department of Genetics and Microbiology, University of Pavia, via Abbiategrasso 207, 27100 Pavia, Italy, the §Department of Biomolecular Mass Spectrometry, Bijvoet Center for Biomolecular Research and Utrecht Institute for Pharmaceutical Sciences, Utrecht University, 3584 CA Utrecht, The Netherlands, the ‖Laboratory of Biochemistry, Wageningen University, Dreijenlaan 3, 6703 HA Wageningen, The Netherlands, and **Medical Research Council France, European Synchrotron Radiation Facility, Boîte Postale 220, 38043 Grenoble CEDEX, France*

The catabolism of toxic phenols in the thermophilic organism *Bacillus thermoglucosidasius* A7 is initiated by a two-component enzyme system. The smaller flavin reductase PheA2 component catalyzes the NADH-dependent reduction of free FAD according to a ping-pong bisubstrate-biproduct mechanism. The reduced FAD is then used by the larger oxygenase component PheA1 to hydroxylate phenols to the corresponding catechols. We have determined the x-ray structure of PheA2 containing a bound FAD cofactor (2.2 Å), which is the first structure of a member of this flavin reductase family. We have also determined the x-ray structure of reduced holo-PheA2 in complex with oxidized NAD (2.1 Å). PheA2 is a single domain homodimeric protein with each FAD-containing subunit being organized around a six-stranded β-sheet and a capping α-helix. The tightly bound FAD prosthetic group (K_d = 10 nM) binds near the dimer interface, and the *re* face of the FAD isoalloxazine ring is fully exposed to solvent. The addition of NADH to crystalline PheA2 reduced the flavin cofactor, and the NAD product was bound in a wide solvent-accessible groove adopting an unusual folded conformation with ring stacking. This is the first observation of an enzyme that is very likely to react with a folded compact pyridine nucleotide. The PheA2 crystallographic models strongly suggest that reactive exogenous FAD substrate binds in the NADH cleft after release of NAD product. Nanoflow electrospray mass spectrometry data indeed showed that PheA2 is able to bind one FAD cofactor and one FAD substrate. In conclusion, the structural data provide evidence that PheA2 contains a dual binding cleft for NADH and FAD substrate, which alternate during catalysis.

* This work was supported in part by grants from the Ministero della Università e Ricerca Scientifica e Tecnologica (Progetto "Biologia strutturale e dinamica di proteine redox") and by Grant CQLK CT 725 from the European Union. BM14 is supported by the United Kingdom Research Councils. The costs of publication of this article were defrayed in part by the payment of page charges. This article must therefore be hereby marked "*advertisement*" in accordance with 18 U.S.C. Section 1734 solely to indicate this fact.

The atomic coordinates and structure factors (code 1RZ0 and 1RZ1) have been deposited in the Protein Data Bank, Research Collaboratory for Structural Bioinformatics, Rutgers University, New Brunswick, NJ (http://www.rcsb.org/).

¶ Supported by Marie Curie Fellowship HPMF-CT-2000-00786 from the European Community. To whom correspondence may be addressed. E-mail: r.h.h.vandenheuvel@chem.uu.nl.

‡‡ To whom correspondence may be addressed. E-mail: mattevi@ipvgen.unipv.it.

The non-enzymatic reduction of free flavins by reduced pyridine nucleotides is known to be a rather slow process. Therefore, microorganisms have evolved flavin reductases (NAD(P)H:flavin oxidoreductases) that catalyze the reduction of riboflavin, FMN, or FAD by NADH or NADPH (1). Although the biological function of reduced flavins is not well understood, it is suggested that they play an important role as redox mediators in iron uptake and metabolism in prokaryotes or in light emission in the bioluminescence reaction of bacteria (2–4).

On the basis of amino acid sequences we can distinguish three subgroups of flavin reductases. Members of the first class are found in *Escherichia coli* and luminous bacteria, like *Vibrio fischeri* and *Vibrio harveyi* (5–7). The LuxG protein class is found in *lux* operons and shows significant sequence homology with the members of the first class (5). In recent years, a third class of flavin reductases has been identified, whose members act in combination with a flavin-dependent oxygenase for oxidation of the substrate by molecular oxygen (8–15). These short-chain flavin reductases do not have amino acid sequence homology with the members of the first two classes and are involved in a variety of biological reactions such as the oxidation of aromatic compounds (12, 15), the degradation of chelating agents (10), the desulfurization of fossil fuels (13), and the biosynthesis of antibiotics (8, 9, 11). In these two-component enzymes, the reduced flavin substrate, originating from the flavin reductase, reacts with molecular oxygen in the active site of the oxygenase to produce a putative flavin hydroperoxide intermediate, which in turn can oxidize the substrate (8–14). Thus, these enzymes carry out their reductive and oxidative half-reactions in two separate polypeptide chains. In the case of 4-hydroxyphenylacetate 3-monooxygenase the reductase and oxygenase components do not need to interact for the hydroxylation of 4-hydroxyphenylacetate (12).

Recently, it has been shown that the initial conversion of phenol into catechol by the thermophilic microorganism *Bacillus thermoglucosidasius* A7 is carried out by two protein components encoded by the *pheA1* and *pheA2* genes (15–17). The larger oxygenase component PheA1[1] has a molecular mass of 57 kDa and shares significant amino acid sequence identity with the oxygenase component of 4-hydroxyphenylacetate monooxygenases (12), phenol hydroxylase from *Bacillus thermo-*

[1] The abbreviations used are: PheA1, oxygenase component of phenol hydroxylase from *Bacillus thermoglucosidasius* A7; PheA2, flavin reductase component of phenol hydroxylase from *Bacillus thermoglucosidasius* A7.

leovorans A2 (17), and 2,4,6-trichlorophenol 4-monooxygenase from *Pseudomonas pickettii* (18). The smaller flavin reductase component PheA2 has a molecular mass of 17.6 kDa and shares high amino acid sequence identity with a large number of short-chain flavin reductases (8–13, 15). Very recent biochemical data have shown that PheA2 catalyzes the NADH-dependent reduction of free flavins according to a ping-pong bisubstrate-biproduct catalytic mechanism (15). The formed reduced flavins react with PheA1 to catalyze the *ortho*-hydroxylation of simple phenols into the corresponding catechols.

To date, no structural information is available for any of the members of the two-component flavoprotein monooxygenase family. PheA2 homologues share weak amino acid sequence identity (<20%) with the archaeal ferric reductase from *Archaeoglobus fulgidus* (19) from which the x-ray structure has recently been determined (20). This enzyme catalyzes the flavin-mediated reduction of ferric iron complexes using NAD(P)H as electron donor. Both biochemical and structural data have shown that the flavin substrate binds only weakly to the enzyme. Intriguingly, ferric reductase uses its single domain to bind both FMN and NAD(P)H and does not contain the Rossmann fold to bind the NAD(P)H molecule (20).

Here, we present three-dimensional structures of flavin reductase PheA2 from *B. thermoglucosidasius* A7 in complex with FAD (2.2 Å) and in complex with reduced FAD and NAD (2.1 Å) solved by x-ray crystallography. The bound NAD product adopts an unusual folded conformation in PheA2. On the basis of these crystallographic data and additional electrospray ionization mass spectrometry and fluorescence binding studies we conclude that flavin reductase PheA2 contains a flavin cofactor and an additional binding groove for binding NADH and flavin substrate, which alternate during catalysis. These structural data fully support the proposed ping-pong bisubstrate-biproduct mechanism of action.

EXPERIMENTAL PROCEDURES

Protein Expression, Purification, and Analytical and Crystallization Procedures—The *pheA2* gene from *B. thermoglucosidasius* A7 encoding PheA2 was overexpressed in the *E. coli* strain BL21(DE3)pLysS at 30 °C in Luria-Bertani medium in the absence of isopropyl β-D-thiogalactopyranoside as described previously (16, 21). To obtain the selenomethionine-substituted PheA2, the *pheA2* gene was transformed in *E. coli* BL21(DE3)pLysS (16). To favor the production of selenomethionine-substituted protein, the biosynthesis of native protein was blocked by using growth medium without L-methionine. Specifically, *E. coli* containing the *pheA2* gene was grown in a minimal M9 medium (8 g/liter dibasic sodium phosphate, 4 g/liter monobasic potassium phosphate, 0.5 g/liter sodium chloride, and 0.5 g/liter ammonium chloride, pH 7.4) (22) supplemented with 50 mg/liter L-amino acids except L-methionine, 100 mg/liter seleno-DL-methionine, 0.1 mM calcium chloride, 1 mM magnesium sulfate, 1 mM thiamine, 2 g/liter glucose, 1 mg/liter riboflavin, 1 mg/liter niacinamide, 1 mg/liter pyridoxin, and 75 mg/liter ampicillin. The *E. coli* cells were grown at 30 °C for 2 days in the absence of isopropyl β-D-thiogalactopyranoside.

Native PheA2 and selenomethionine-substituted PheA2 were purified according to the procedure established by Kirchner *et al.* (15) with minor modifications. *E. coli* cells were resuspended in 50 mM sodium phosphate buffer, 0.5 mM ethylenediaminetetraacetic acid, 0.5 mM phenylmethanesulfonyl fluoride, and 0.5 mg DNase, pH 7.0. After disruption of the cells by sonication and removal of cell debris, the protein sample was treated with 0.5% (w/v) protamine sulfate followed by the addition of 1.4 M ammonium sulfate. The protein was then loaded onto a phenyl-Sepharose column (10 × 2.6 cm) equilibrated in 50 mM sodium phosphate buffer, 1.3 M ammonium sulfate, and 0.5 mM EDTA, pH 7.0. PheA2 was eluted with a linear descending gradient from 1.3 to 0.4 M ammonium sulfate and dialyzed against the sodium phosphate buffer without ammonium sulfate. The dialyzed protein sample was loaded onto a Q-Sepharose column (10 × 2.6 cm) pre-equilibrated with 50 mM sodium phosphate and 0.5 mM EDTA, pH 7.0. PheA2 was eluted with a linear ascending gradient from 0 to 0.6 M NaCl. The protein was then loaded onto a preparative Superdex 75 (60 × 1.6 cm) column pre-equilibrated with 50 mM sodium phosphate buffer and 0.5 mM EDTA, pH 7.0. Pure PheA2 fractions were pooled and frozen at −80 °C. PheA2 apoprotein was prepared by treating the enzyme with 2.5 M guanidinium hydrochloride in 50 mM potassium phosphate buffer, pH 7.0. The FAD prosthetic group was removed by eluting the protein sample over a Biogel P-6 DG size-exclusion chromatography column equilibrated with 50 mM sodium phosphate buffer and 2.5 M guanidium hydrochloride, pH 7.0.

All analytical experiments were performed in sodium phosphate buffer, pH 7.0, at 25 °C unless stated otherwise. Fluorescence emission spectra were recorded on an SLM-Aminco SPF 500C fluorescence spectrophotometer. Dissociation constants of apoenzyme·flavin complexes were determined from fluorescence titration experiments with excitation set at 450 nm. Steady-state fluorescence anisotropy experiments were performed on a home-built fluorescence spectrophotometer equipped with two photomultipliers arranged in T-format (Thorn EMI 9863QA/350, operating in photon-counting detection mode) as described previously (23). NADH oxidase activity was determined spectrophotometrically by monitoring the decrease in absorption of NADH at 340 nm (ϵ_{340} = 6.22 mM^{-1} cm^{-1}) at 40 °C. The assay mixture routinely contained 0.2 mM NADH and 0.01 mM FAD. To determine the specificity of the reaction, FMN, riboflavin, and NADPH were also tested as substrates. Absorption spectra were recorded using a Hewlett Packard 8453 diode-array spectrophotometer.

For nanoflow electrospray mass spectrometry experiments 4 μM PheA2 was prepared in aqueous 10 mM ammonium bicarbonate buffer, pH 8.0, and mixed with different concentrations of FAD in the same buffer. The protein was introduced in a nanoflow electrospray mass spectrometer coupled to an orthogonal time-of-flight analyzer operating in positive ion mode (Micromass LC-T, Waters). The electrospray voltages applied were optimized for optimal transmission of the PheA2 ions (capillary voltage 1300–1350 V and cone voltage 60 V). Borosilicate glass capillaries (Kwik-Fil, World Precision Instruments) were used on a P-97 puller (Sutter Instruments) to prepare the nanoflow electrospray capillaries with an orifice of about 5 μm. The capillaries were subsequently coated with a thin gold layer using an Edwards Scancoat six Pirani 501 sputter coater (Edwards High Vacuum International).

Crystals of PheA2 were grown at 20 °C by the hanging drop, vapor diffusion method. The hanging drops contained 4 μl of an equal mixture of protein solution (16 mg/ml PheA2 in 50 mM sodium phosphate buffer, pH 7.0) and reservoir solution (20–26% polyethylene glycol 3350 and 0.4 M magnesium nitrate). Hanging drops were allowed to equilibrate against 1 ml of reservoir solution for several days. Bright yellow crystals appeared with overall dimensions of 0.5 × 0.4 × 0.1 mm. NAD-complexed enzyme was prepared by soaking the enzyme crystals in the reservoir solution containing 5 mM NADH for 1 h at 20 °C. Bleaching of the FAD cofactor indicated that NADH reacted with the crystalline enzyme resulting in the accumulation of reduced FAD in the crystals.

X-ray Data Collection and Processing—PheA2 crystals were cryocooled by plunging into liquid nitrogen, and x-ray data were collected at 100 K using a nitrogen stream. Cryoprotection was accomplished by placing the PheA2 crystals for a few s in a cryoprotectant solution (26% polyethylene glycol 3350, 0.4 M magnesium nitrate, and 25% (w/v) glycerol). Data from the selenomethionine-substituted PheA2 were collected on beamline BM14 at the European Synchrotron Radiation Facility (Grenoble, France) using a MarCCD detector. The two data sets (at 0.97917 and 0.88570 nm for peak and remote, respectively) were processed using MOSFLM (24) and the CCP4 suite of programs (25). The selenomethionine PheA2 crystals belong to space group $P2_1$ with eight protein chains in the asymmetric unit.

Structure Determination, Model Building, and Refinement—The initial sites of the anomalous scattering atoms were found using the program ShelxD (26) using the peak data. ShelxD detected 48 atoms, corresponding to eight monomers (8 × 6 selenomethionines including the N-terminal selenomethionine residue)/asymmetric unit. The initial sites were refined and employed in phasing using the program ShelxE (26). The phases were further improved by 8-fold non-crystallographic symmetry averaging and solvent flattening using the program DM (27). The resulting electron density map was of excellent quality. A summary of the data collection and phasing statistics is presented in Table I.

The automated model-building application of the program ARP (28) was used for protein model building. Following the standard protocol suggested by the authors, a total of 1151 of 1224 peptides were traced (94%). The subsequent refinement of this initial model consisted of alternating rounds of manual fitting of the model to electron density maps using the program O (29) and maximum likelihood refinement with REFMAC (30). Two percent of the data were set aside to compute R_{free} (31). Ordered water molecules were added using the standard

TABLE I
Statistics for x-ray data collection

Data collection	PheA2		PheA2·NAD
	Selenomethionine peak	Selenomethionine remote	
Wavelength (Å)	0.97917	0.88570	
Space group	$P2_1$	$P2_1$	$P2_1$
Cell parameters	a = 53.75 Å b = 155.00 Å c = 84.27 Å β = 91.45°	a = 53.77 Å b = 155.14 Å c = 84.28 Å β = 91.36°	a = 53.69 Å b = 156.45 Å c = 83.92 Å β = 91.10°
Resolution range[a] (Å)	15.0–2.2 (2.26–2.2)	15.0–2.2 (2.26–2.2)	15–2.1 (2.15–2.1)
Observed reflections	215,737	122,181	167,477
Unique reflections	68,747	66,610	77,418
Completeness[a] (%)	98.6 (98.0)	95.5 (94.2)	96.3 (98.7)
R_{merge}[a,b] (%)	7.4 (24.2)	6.6 (20.4)	9.6 (49.8)
Intensities[a] ($\langle I/\sigma(I)\rangle$)	6.9 (2.9)	8.3 (3.6)	7.2 (1.1)
MAD phased map: contrast/connectivity[c]	0.64/0.89		

[a] Numbers in parentheses correspond to data in the outermost resolution shell.
[b] $R_{merge} = \Sigma|I_j - \langle I_j\rangle|/\Sigma\langle I_j\rangle$, where I_j is the intensity of an observation of reflection j and $\langle I_j\rangle$ is the average intensity for reflection j.
[c] Calculated with ShelxE (26).

protocol of the solvent-building application of the program ARP (28). Refinement statistics are shown in Table II. The final model of selenomethionine-substituted holo-PheA2 consists of eight polypeptide chains with a total of 1224 residues (residues 1–153; residues 154–160 are disordered in all eight crystallographically independent monomers), eight FAD molecules, and 407 water molecules. Of the amino acids 91.5% are in the core region of the Ramachandran plot (32), and no residues are in the generously allowed and disallowed regions.

The initial phases of the holo-PheA2·NAD structure were obtained by rigid-body refinement using the program REFMAC with the 2.2-Å holo-PheA2 structure serving as the starting model. The water molecules were removed prior to refinement calculations. The initial map showed very clear electron density for NAD bound in a folded conformation. After rigid-body refinement, the structure of NADH-soaked PheA2 was refined as described for native PheA2. The final model consists of a total of 1224 residues, eight reduced FAD cofactors, eight NAD molecules, and 397 water molecules. 92.4% of the amino acids are in the core region of the Ramachandran plot (32), and no residues are in the generously allowed and disallowed regions. Pro-43 is in the *cis* conformation in all eight PheA2 monomers of both x-ray models.

Amino acid sequence similarity searches were performed with PSI-BLAST (33), and multiple sequence alignments were made using ClustalX (34). Analyses of the three-dimensional structure and model superpositions were carried out with O (29), MSMS (35), and DALI (36). Drawings were produced with LIGPLOT (37), MOLSCRIPT (38), DINO,[2] and Raster3D (40).

TABLE II
Refinement statistics for final models

	PheA2	PheA2·NAD
R_{factor}[a] (%)	22.3	23.7
R_{free}[a] (%)	25.3	25.6
Number of total atoms	10,239	10,581
FAD molecules	8	8
NAD molecules	0	8
Water molecules	407	397
Root mean square deviation bond length (Å)	0.017	0.015
Root mean square deviation bond angle (°)	1.4	1.5
Average B value (Å^2)	31.3	34.4
Ramachandran statistics[b]	91.5/8.5/0.0/0.0	92.4/7.6/0.0/0.0

[a] $R_{factor} = \Sigma\,\|\|F_{obs}| - |F_{calc}\|/\Sigma|F_{obs}|$, R_{free} for 2% subset of reflections not included in the refinement (31).
[b] Number of residues in most favored, additional allowed, generously allowed, and disallowed regions, respectively (32).

RESULTS AND DISCUSSION

Three-dimensional Structure of PheA2—The x-ray structure of the selenomethionine-substituted PheA2 was solved in complex with the non-covalent cofactor FAD at 2.2-Å resolution and in complex with the reduced FAD cofactor and oxidized NAD product at 2.1-Å resolution. The two described structures are highly similar to each other with a root mean square deviation of only 0.23 Å for 153 Cα atoms (as calculated for monomer A). The monoclinic PheA2 crystals contain four homodimers in the asymmetric unit. The two subunits forming the homodimer are related by a molecular 2-fold rotation axis (Fig. 1*A*). The eight monomers, of both x-ray models, in the asymmetric unit are essentially identical with root mean square deviations of lower than 0.2 Å for all Cα atoms. The secondary structure of the enzyme consists of eleven β-strands and three α-helices. Structurally the most similar proteins in the Protein Data Bank are the FMN-binding protein from *Methanobacterium thermoautotrophicum* (Protein Data Bank accession code 1EJE) (41), the FMN-binding protein from *Desulfovibrio vulgaris* (Protein Data Bank accession code 1AXJ) (42), and ferric reductase from *A. fulgidus* (Protein Data Bank accession code 1IOR) (20) with root mean square deviations of 2.4 Å for 149 Cα atoms, 3.1 Å for 89 Cα atoms, and 2.1 Å for 140 Cα atoms, respectively. Like these three proteins, the core of the PheA2 subunit consists of a six-stranded antiparallel β-barrel with a capping α-helix that contacts the ribityl phosphate of the FAD molecule. It is recognized that the β-barrel is a circular permutation of the flavin binding domain of the ferredoxin reductase superfamily (43, 44). Members of the ferredoxin reductase superfamily contain, in addition to the flavin binding domain, a second Rossmann fold domain, which is used to bind the pyridine nucleotide NADH or NADPH (44). PheA2 and ferric reductase (20) bind the pyridine nucleotides as well; however, they lack the Rossmann fold domain. Indeed, our crystallographic analysis of PheA2 in complex with NAD (see below) and the crystallographic model of ferric reductase in complex with NADP (20) show that pyridine nucleotide coenzymes bind to these single domain enzymes.

PheA2 and ferric reductase have a similar overall fold, but we observed between the two x-ray models some important structural differences that are related to their biological function. Whereas ferric reductase catalyzes the flavin-mediated reduction of ferric iron complexes (19, 45), PheA2 does not react with these ferric complexes (15). The ferric reductase crystallographic model has suggested a ferric complex binding site, which is formed by Thr-31, Leu-35, Cys-45, and His-126 (20). His-126 is conserved in PheA2 (His-123) and most other short-chain flavin reductases. The remaining three residues (Thr-31, Leu-35, and Cys-45), however, are neither conserved in PheA2 (Ala-35, Val-39, and Ser-49) nor in the short-chain flavin reductase family members. A second important difference be-

[2] DINO (2002) www.dino3d.org.

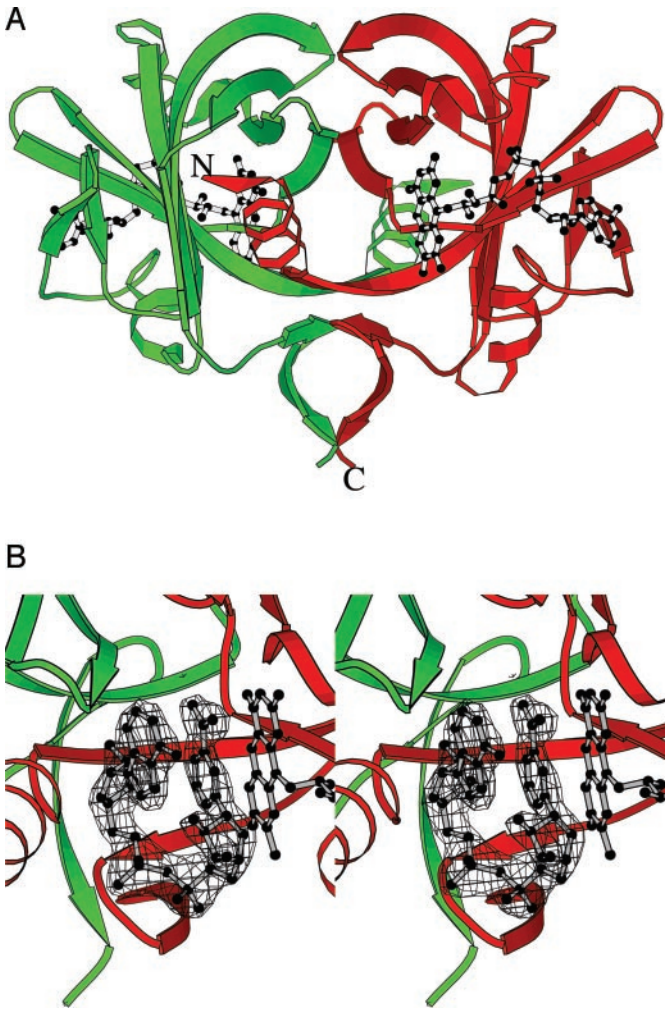

FIG. 1. **X-ray model of PheA2 and binding of FAD and NAD to the enzyme.** *A*, ribbon representation of the PheA2 dimer viewed perpendicular to the dimer 2-fold axis. The two monomers are depicted in *green* and *red*. The FAD cofactor is drawn in a ball-and-stick representation. *B*, stereoview presentation of the binding mode of NAD and reduced FAD to PheA2. This figure shows that NAD binds to PheA2 in a highly folded conformation with the nicotinamide ring stacked onto the adenine ring in a nearly parallel fashion. In turn, the isoalloxazine ring of reduced FAD is packed in parallel against the nicotinamide of NAD. The $2F_o - F_c$ electron density map of NAD was calculated with the phases from the final model omitting the atoms for NAD. The contour level is 1 σ.

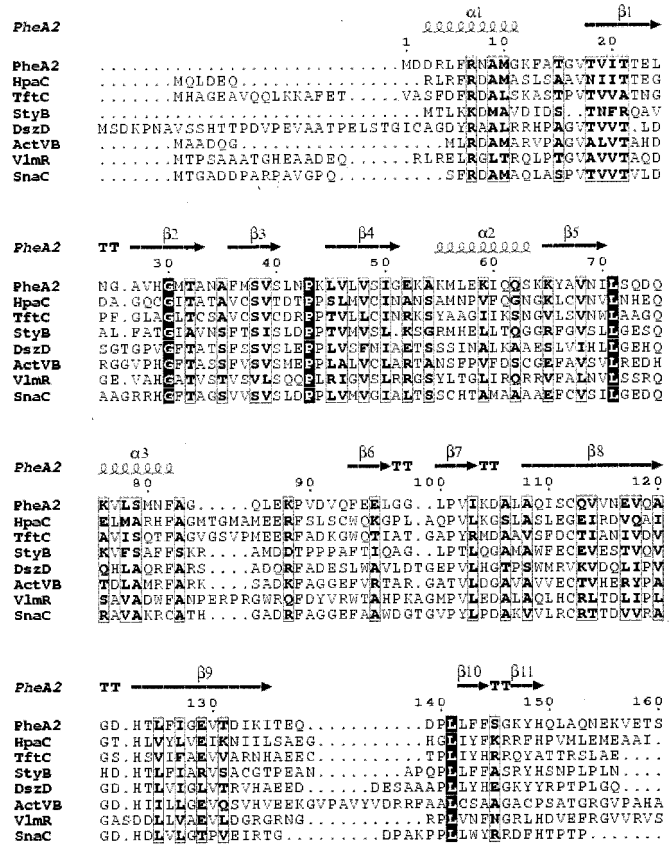

FIG. 2. **Amino acid sequence alignment of PheA2 with two-component flavin reductases.** Abbreviations and accession numbers for the proteins are as follows: PheA2, phenol 2-hydroxylase component B from *B. thermoglucosidasius* A7 (gi 7672525); hpaC, 4-hydroxyphenylacetate hydroxylase component C from *E. coli* (gi 6983686); tftC, chlorophenol 4-monooxygenase component 2 from *Burkholderia cepacia* (gi 21954029); styB, styrene monooxygenase component 2 from *Pseudomonas* sp. (gi 2598027); dszD, NAD(P)H:FMN oxidoreductase from *Rhodococcus erythropolis* (gi 2944380); actVB, actinorhodin polyketide dimerase component B from *Streptomyces coelicolor* (gi 14717099); vlmR, NADPH oxidoreductase from *Streptomyces viridifaciens* (gi 1711412); and snaC, NAD(P)H:FMN oxidoreductase from *Streptomyces pristinaespiralis* (gi 1711412). The PheA2 secondary structure is shown above the alignment with α-helices, β-strands, and turns. Conserved amino acids are shown in *boxes*, and identical amino acids are shown with a *black background*.

tween PheA2 and ferric reductase concerns the reactivity toward and binding of flavin molecules. PheA2 contains a tightly bound FAD cofactor (see below) (15), whereas ferric reductase uses a weakly bound FMN (19, 20). It is noteworthy that crystalline ferric reductase binds only one FMN (and NADP)/dimer. The differences between PheA2 and ferric reductase may be (partially) related to loop 7. This polypeptide stretch, positioned between α-helix 3 and β-strand 6, is involved in binding of FAD and FMN in PheA2 and ferric reductase, respectively. Loop 7 in the FMN-complexed ferric reductase model is highly ordered, whereas this loop becomes flexible in the absence of FMN. Loop 7 in PheA2 is shifted by >10 Å, such that the AMP moiety of FAD can fit in the PheA2 structure. The amino acid sequence of loop 7 in PheA2 is not conserved within ferric reductase from *A. fulgidus* (15) nor in any related short-chain flavin reductase (Fig. 2). Moreover, the loop is not present in the flavin binding domain of the ferredoxin reductase superfamily (44).

Description of the FAD Binding Site in PheA2—The FAD molecule in PheA2 is bound in a wide groove of the protein with the isoalloxazine ring positioned at the dimer interface (Fig. 1*A*). The *si* face of the FAD isoalloxazine ring is buried and contacting the β2 strand; however, the *re* face is completely exposed to bulk solvent (Fig. 3*A*). The 2,4-pyrimidinedione moiety of the isoalloxazine ring forms an extensive hydrogen bond network with the main chain atoms of residues Asn-34, Ala-35, Ser-49, and Gly-51 and a water molecule (Fig. 3*B*). Moreover, the main chain nitrogen atom of Asn-34 is hydrogen-bonded to FAD N5. The dimethylbenzene portion of the isoalloxazine ring sits in a hydrophobic pocket formed by Ala-33, Ala-83, and Phe-143. The pyrophosphate moiety of FAD is hydrogen-bonded to the main chain atoms of residues Thr-32, Lys-55, and Met-56 and two water molecules. The FAD ribose and adenine moieties form hydrogen bond interactions with Val-28 and Asn-81, and some hydrophobic interactions exist between this part of the FAD molecule and residues of the described loop 7. Taken together, FAD is stabilized by 11 hydrogen bonds with the protein and four potential hydrogen bonds with water molecules, and the *re* face of the isoalloxazine ring of FAD is exposed to bulk solvent. Only one hydrogen bond interaction with the protein involves an amino acid side chain

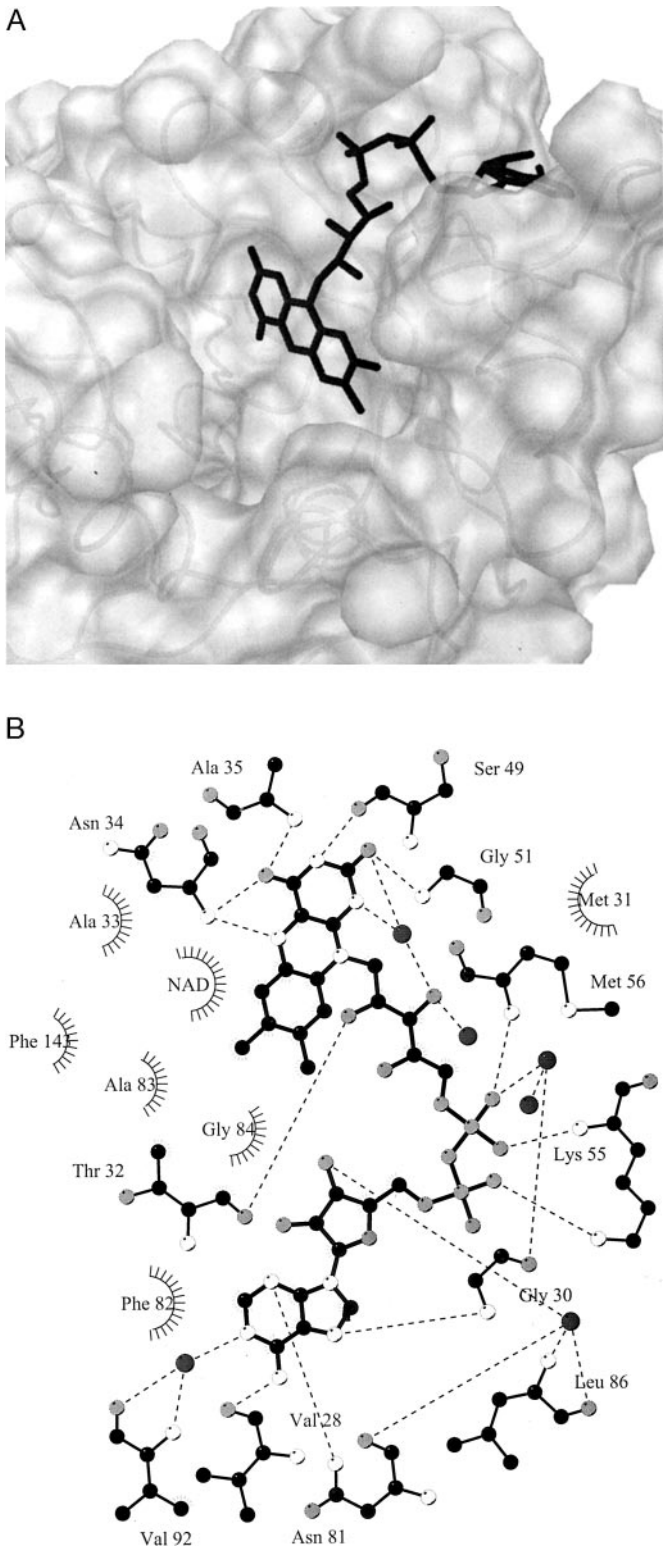

FIG. 3. **Binding of FAD cofactor to PheA2.** *A*, the binding site of FAD in PheA2 is such that the *re* face of the isoalloxazine ring is exposed to solvent. The solvent-accessible area was calculated with MSMS (35). *B*, schematic of hydrogen bond patterns between PheA2 and FAD. Potential hydrogen bonds between FAD and the protein and between FAD and water molecules are indicated by *dashed lines*.

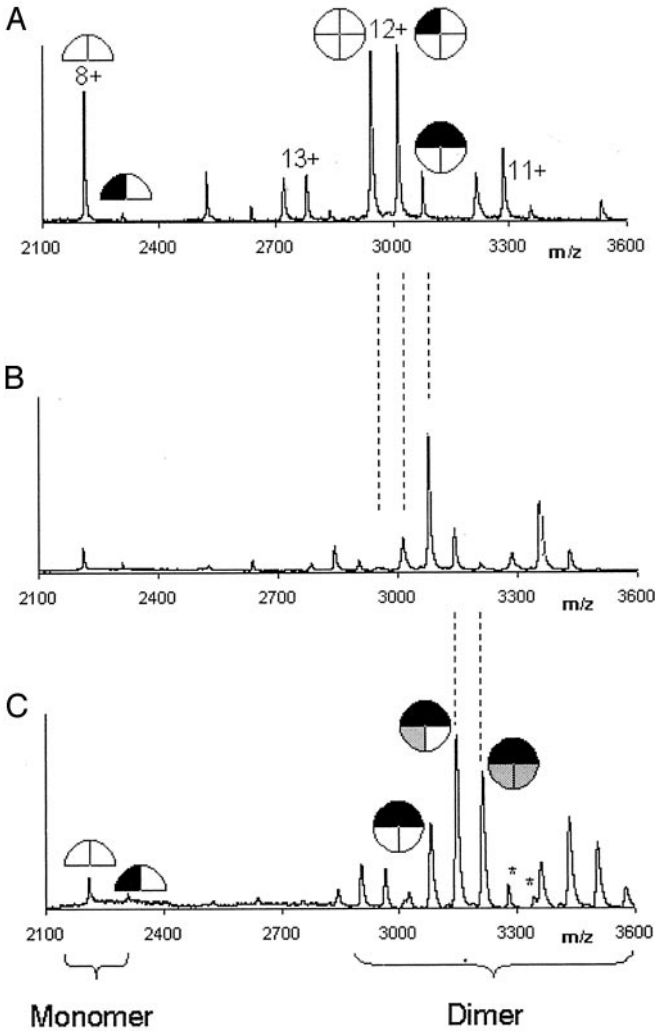

FIG. 4. **Nanoflow electrospray mass spectra of PheA2 with added FAD.** 4 μM holo-PheA2 in 40 mM ammonium bicarbonate, pH 8.0, was mixed with 0 μM FAD (*A*), 40 μM FAD (*B*), and 100 μM FAD (*C*). Monomeric and dimeric species are shown as are the charge states of the most abundant protein ions. FAD cofactor and substrate binding are indicated in *black* and *gray*, respectively.

(Asn-81 ND2), whereas all other hydrogen bonds involve main chain atoms.

The observed binding mode of FAD in PheA2 suggests that the dimeric protein form is most likely essential for flavin binding. Indeed, the FAD site is juxtaposed to the dimer interface, although there is no direct contact between FAD and a residue of the 2-fold related subunit. Therefore, we investigated flavin binding to monomeric and dimeric PheA2. Presently, mass spectrometry is a well accepted tool to study interactions between protein and ligands. In particular nanoflow electrospray ionization mass spectrometry transfers molecules gently from solution phase into gas phase, enabling the analysis of intact protein·ligand complexes (46–49). The average molecular mass of PheA2 determined from the nanoflow electrospray mass spectra was 17,660 ± 4 Da and 35,325 ± 6 Da for monomeric and dimeric apo-PheA2, respectively (Fig. 4). This mass is in close agreement with the mass as calculated from the PheA2 amino acid sequence (17,660 Da) (16). The obtained mass spectra clearly showed that in the gas phase, even upon adding a 25-fold excess of FAD, the monomeric form was mainly present as the apoprotein. In contrast, the dimeric form was mainly present as the holoprotein (*i.e.* PheA2 in complex with FAD cofactor) upon adding a 10-fold excess of FAD (Fig. 4). These results are fully consistent with the FAD being bound to the enzyme near the interface between the two monomers.

Flavin reductases belonging to the family of PheA2 display only weak binding of riboflavin, FMN, or FAD (12, 50). During the purification procedure of PheA2, however, we never ob-

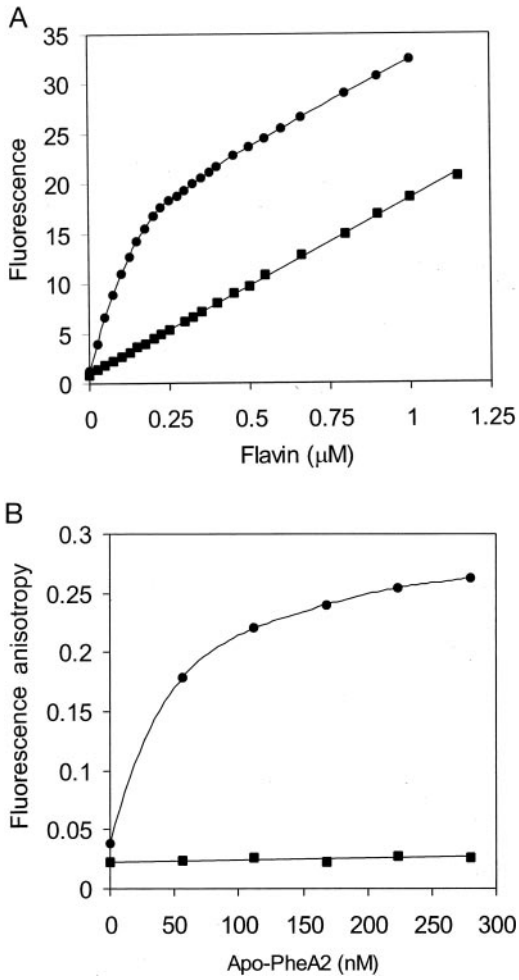

FIG. 5. **Binding of FAD and FMN to PheA2.** *A*, fluorescence changes upon titration of 170 nM PheA2 apoprotein with FAD (●) or FMN (■) in 50 mM potassium phosphate buffer, pH 7.0. The fluorescence emission was measured at 530 nm upon excitation at 450 nm. *B*, fluorescence anisotropy changes upon titration of 210 nM FAD (●) or 210 nM FMN (■) with PheA2 apoprotein in 50 mM potassium phosphate buffer, pH 7.0. The fluorescence anisotropy of PheA2 holoprotein is 0.27.

served any release of FAD, suggesting tight binding to the enzyme. Moreover, FAD was well defined within the electron density, pointing toward a high affinity of the enzyme for the flavin. To determine the binding affinity of the enzyme for FAD we prepared PheA2 apoprotein. Upon size-exclusion chromatography in the presence of 4 M urea, no loss of the flavin was observed. However, PheA2 apoprotein with negligible residual activity could be prepared by size-exclusion chromatography in 2.5 M guanidinium hydrochloride. After dialysis against potassium phosphate buffer, pH 7.0, the PheA2 activity was fully restored by the addition of an excess of FAD. From fluorescence titration experiments of PheA2 apoprotein with FAD we estimated a dissociation constant, K_d = 9.8 ± 0.2 nM, for the apoenzyme·FAD complex (Fig. 5*A*). When FMN was used in the titration experiments, no deviation from fluorescence linearity was observed (Fig. 5*A*), indicating that PheA2 does not tightly interact with FMN. This was corroborated by steady-state fluorescence anisotropy experiments. When FMN was titrated with PheA2 apoprotein no change in fluorescence anisotropy occurred (Fig. 5*B*). Titration of FAD with the apoprotein caused a large increase in fluorescence anisotropy (Fig. 5*B*), approaching the value of the holoprotein. This change in fluorescence is indicative of the longer rotational relaxation time of protein-bound FAD compared with free FAD (51). In summary, PheA2

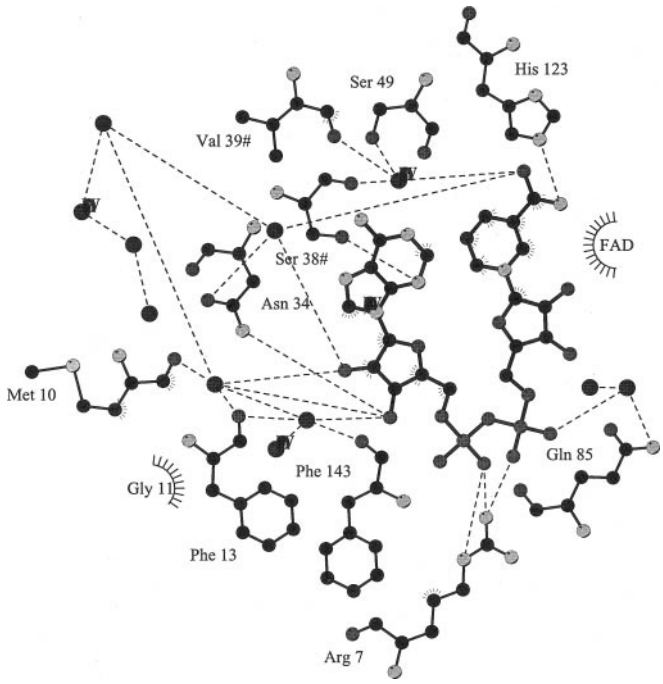

FIG. 6. **Schematic of hydrogen bond patterns between PheA2 and NAD product.** Potential hydrogen bonds between NAD and the protein are indicated by *dashed lines*. # indicates residues from polypeptide chain B.

contains a tightly bound FAD cofactor, which is highly unlikely to be released during catalysis.

The Coenzyme NAD(H) Is Bound to PheA2 in an Unusual Folded Conformation—Kinetic studies have shown that NADH (K'_m = 9 μM) is preferred over NADPH (K'_m > 500 μM) as coenzyme for hydride transfer to the FAD cofactor in PheA2 (15). We soaked 5 mM NADH with PheA2 crystals with the aim to trap a complex between PheA2 and NAD(H). In agreement with solution studies, we observed bleaching of the FAD cofactor upon adding excess of NADH to crystalline PheA2, indicating that the added NADH was able to reduce the enzyme-bound FAD. Thus, PheA2 is active in the crystalline form. However, flavin bleaching did not occur with lower concentrations of NADH (0.5–2 mM), which suggests weak binding of NADH.

The crystallographic model of reduced holo-PheA2 in complex with NAD is highly similar to the native enzyme. NAD is bound in a wide groove and adopts a very compact folded conformation with the nicotinamide ring stacked over the adenine base in a nearly parallel mode. The distance between the adenine C6 and nicotinamide C2 atoms, a general measure for the compactness of NAD(P), is 3.8 Å (Fig. 1*B*) (52). The nicotinamide ring of NAD is packed in a parallel mode against the *re* face of the isoalloxazine ring of FAD with a distance of 3.2 Å between FAD N5 and nicotinamide C4. This distance allows hydride transfer between NADH and FAD. The NAD is lined by the N-terminal α-helix (α1) and residues 32–40 of the β-sheets (β2 and β3) of the 2-fold related chain of the dimer. The bound NAD is hydrogen-bonded to the protein via the side chains of Arg-7 and His-123 and to the side chain of Ser-38 of the opposite polypeptide chain (Fig. 6). In addition, NAD forms a few hydrogen bond interactions with water molecules present in the wide groove. The relatively low number of interactions between the protein and the pyridine nucleotide substrate is in perfect agreement with the rather low binding affinity as observed in kinetic studies (15).

Unlike the folded NAD conformation in PheA2, most enzyme-bound NAD molecules rather adopt an extended confor-

mation. To the best of our knowledge a folded conformation of protein-bound NAD is only observed in two other enzymes, namely in flavin reductase P (53) and in NadR (54). In the x-ray structure of flavin reductase P in complex with NAD, the pyridine nucleotide adopts a folded conformation, similar to that of NAD in PheA2, with an inter-ring distance between the adenine and nicotinamide ring of 3.6 Å. However, NAD is an inhibitor of flavin reductase P rather than a product as for PheA2. The crystallographic model of NadR revealed a NAD molecule bound to a site distinct from the catalytic center. Within this observed NAD conformation the distance between the adenine and nicotinamide ring is 3.8 Å. The function of binding of this NAD molecule is unknown, but the specific interactions between the protein and NAD suggest that binding has at least some biological implications.

The folded NAD conformations described above are proposed to exist in aqueous and some hydrophilic organic environments (55). In these solutions NAD adopts a conformation in which the distance between the nicotinamide and adenine rings is about 4–5 Å. In fact, it is postulated that a hydrophobic environment is important for stabilizing the extended unfolded conformations of NAD (55). Since NAD in PheA2 is bound in an open bulk solvent-accessible cleft this explains the folded conformation of NAD in this enzyme. This is the first observation that suggests that an enzyme can react with a folded compact pyridine nucleotide, implying that an extended conformation is not required for catalysis (55). Such a folded NADH conformation in PheA2 has also mechanistic implications in that it creates a solvent-protected microenvironment allowing hydride transfer from the coenzyme to FAD. Interestingly, the conformation of NADP in the homologous ferric reductase is different from that found in PheA2 in that it is more extended with no stacking between adenine and nicotinamide rings. This difference between PheA2 and ferric reductase is likely to be explained by different conformations of the N-terminal (1–15) and C-terminal (140–153) residues, which surround the active site cleft (20).

Mechanism of Action of PheA2—PheA2 belongs to a novel family of short-chain flavin reductases that act in combination with a flavin-dependent oxygenase for hydroxylation of the substrate by molecular oxygen. The small PheA2 component supplies reduced FAD to the large PheA1 component. The hydroxylation of phenolic compounds by PheA1 strictly depends on $FADH_2$, but PheA2 can also reduce FMN and riboflavin with similar catalytic efficiencies (k_{cat}/K_m) (15). All kinetic data of PheA2 point toward a ping-pong bisubstrate-biproduct kinetic mechanism for transferring free reduced FAD to PheA1 (15).

$$\text{PheA2-FAD}_{ox} + \text{NADH} \rightleftarrows \text{PheA2-FAD}_{red} + \text{NAD}$$

REACTION 1

$$\text{PheA2-FAD}_{red} + \text{FAD}_{ox} \rightleftarrows \text{PheA2-FAD}_{ox} + \text{FAD}_{red}$$

REACTION 2

A fundamental consequence of this mechanism of action is that the NAD product is released before flavin substrate binds. As pointed out above, folded compact NAD is trapped within a wide groove of PheA2 packed against the *re* face of the FAD isoalloxazine ring. The distance between nicotinamide C4 and FAD N5 is 3.2 Å such that hydride transfer between NADH and FAD can occur. According to the proposed reaction mechanism the oxidized NAD would be released and flavin substrate would enter the enzyme. The present PheA2 crystallographic models clearly reveal that reactive binding of FAD substrate to FAD cofactor-complexed PheA2 (holo-PheA2) is only possible in the NADH-binding active site cleft. Extensive attempts to cocrystallize the complex between holo-PheA2 and FAD substrate and soaking of FAD with holo-PheA2 crystals were not successful. We did not attempt to model a flavin substrate into this wide groove because of the large number of freedom degrees in the FAD conformation and the uncertainty of the stereochemistry of the reaction (*i.e.* whether the FAD substrate accepts the hydride anion on its *re* or *si* side). However, the substrate flavin isoalloxazine ring could easily be packed in a catalytically competent conformation against the *re* face of the isoalloxazine ring of the FAD cofactor without any forced movements or steric restraints. By analogy with the folded conformation of NAD, the flavin substrate might adopt a folded conformation similar to that found for FAD bound to DNA photolyase. Again, this would create a solvent-protected microenvironment for optimal electron transfer (39, 56).

With the aim to obtain more information on the binding of flavin substrate to holo-PheA2 we performed nanoflow electrospray mass spectrometry experiments with added FAD (Fig. 4). We verified by absorption spectroscopy that PheA2 was fully saturated with FAD cofactor (holo-PheA2). The mass spectrum of 4 μM holo-PheA2, however, showed that in the gas phase dimeric PheA2 was not fully saturated with FAD cofactor. Instead, about 40% of the protein contained only one FAD molecule and about 40% no FAD molecule. When sprayed from a solution containing up to a 10-fold excess of FAD, mass spectra were obtained that show near saturation of the FAD cofactor to PheA2. Moreover, we observed binding of a third and fourth molecule of FAD to the PheA2 dimer, indicating that PheA2 can bind, next to the FAD cofactor, a FAD substrate molecule. When we added a 25-fold excess of FAD the mass spectra clearly revealed that PheA2 dimer can indeed bind a total of four molecules of FAD (two cofactors and two substrates). We observed some low abundant satellite peaks, suggesting the nonspecific binding of FAD molecules. However, the total peak areas of these latter products were very low. Moreover, the mass spectra of the PheA2 monomer showed, even with a 25-fold excess of FAD, only low abundant peaks of an equimolar complex between PheA2 and FAD, indicating a weak binding site for one molecule of FAD. Thus, the electrospray mass spectra strongly suggest a second, though rather weak, binding site for a flavin substrate in the PheA2 dimer. Taken together, the x-ray crystallography and mass spectrometry data suggest that PheA2 contains a FAD cofactor and a dual binding site for NADH and flavin substrate. These two molecules alternate during catalysis such that reduced flavin substrates are released. Possibly, the binding affinity of the FAD substrate is dependent on the redox state of the enzyme-bound FAD cofactor (*i.e.* the binding of FAD substrate would improve upon reduction of the FAD cofactor).

PheA2 is a unique member of the short-chain flavin reductase family, as it contains FAD as tightly bound cofactor and a flavin molecule as substrate and reacts via a ping-pong bisubstrate-biproduct kinetic mechanism. The structural design of short-chain flavin reductase family members is a rather simple solution for the reduction of flavin molecules by pyridine nucleotides. The interactions between the flavin and protein are too weak to generate a true flavoprotein, and the specificities for both the flavin and the reduced pyridine nucleotide are broad. Thus, flavin reductases can be classified as general reducing systems. PheA2 behaves also as a general reducing system with a low specificity for the final exogenous electron acceptor (FAD), but it has evolved a specific binding site for a FAD cofactor.

Acknowledgments—D. M. E. Jeukens and R. Baron are thanked for excellent technical assistance.

REFERENCES

1. Fontecave, M., Eliasson, R., and Reichard, P. (1987) *J. Biol. Chem.* **262,** 12325–12331
2. Coves, J., and Fontecave, M. (1993) *Eur. J. Biochem.* **211,** 635–641
3. Jeffers, C. E., and Tu, S.-C. (2001) *Biochemistry* **40,** 1749–1754
4. Zenno, S., Saigo, K., Kanoh, H., and Inouye, S. (1994) *J. Bacteriol.* **176,** 3536–3543
5. Ingelman, M., Ramaswamy, S., Nivière, V., Fontecave, M., and Eklund, H. (1999) *Biochemistry* **38,** 7040–7049
6. Koike, H., Sasaki, H., Kobori, T., Zenno, S., Saigo, K., Murphy, M. E., Adman, E. T., and Tanokura, M. (1998) *J. Mol. Biol.* **280,** 259–273
7. Tanner, J. J., Lei, B., Tu, S.-C., and Krause, K. L. (1996) *Biochemistry* **35,** 13531–13539
8. Kendrew, S. G., Harding, S. E., Hopwood, D. A., and Marsh, E. N. (1995) *J. Biol. Chem.* **270,** 17339–17343
9. Parry, R. J., and Li, W. (1997) *J. Biol. Chem.* **272,** 23303–23311
10. Witschel, M., Nagel, S., and Egli, T. (1997) *J. Bacteriol.* **179,** 6937–6943
11. Thibaut, D., Ratet, N., Bisch, D., Faucher, D., Debussche, L., and Blanche, F. (1995) *J. Bacteriol.* **177,** 5199–5205
12. Gálan, B., Diaz, E., Prieto, M. A., and García, J. L. (2000) *J. Bacteriol.* **182,** 627–636
13. Gray, K. A., Pogrebinsky, O. S., Mrachko, G. T., Xi, L., Monticello, D. J., and Squires, C. H. (1996) *Nat. Biotechnol.* **14,** 1705–1709
14. Uetz, T., Schneider, R., Snozzi, M., and Egli, T. (1992) *J. Bacteriol.* **174,** 1179–1188
15. Kirchner, U., Westphal, A. H., Muller, R., and van Berkel, W. J. H. (2003) *J. Biol. Chem.* **278,** 47545–47553
16. Duffner, F. M., Kirchner, U., Bauer, M. P., and Müller, R. (2000) *Gene* (*Amst.*) **256,** 215–221
17. Duffner, F. M., and Müller, R. (1998) *FEMS Microbiol. Lett.* **161,** 37–45
18. Takizawa, N., Yokoyama, H., Yanagihara, K., Hatta, T., and Kiyohara, H. (1995) *J. Ferment. Bioeng.* **80,** 318–326
19. Vadas, A., Monbouquette, H. G., Johnson, E., and Schröder, I. (1999) *J. Biol. Chem.* **274,** 36715–36721
20. Chiu, H.-J., Johnson, E., Schröder, I., and Rees, D. C. (2001) *Structure* **9,** 311–319
21. Studier, F. W., Rosenberg, A. H., Dunn, J. J., and Dubendorff, J. W. (1990) *Methods Enzymol.* **185,** 60–89
22. Ausubel, F. M., Brent, R., Kingston, R. E., Moore, D. D., Seidman, J. G., and Struhl, K. (eds) (1988) *Current Protocols in Molecular Biology*, Lippincott Williams & Wilkins, Philadelphia
23. Engel, M. F., van Mierlo, C. P. M., and Visser, A. J. W. G. (2002) *J. Biol. Chem.* **277,** 10922–10930
24. Leslie, A. G. (1999) *Acta Crystallogr. Sect. D Biol. Crystallogr.* **55,** 1696–1702
25. Collaborative Computational Project Number 4. (1994) *Acta Crystallogr. Sect. D Biol. Crystallogr.* **50,** 760–767
26. Schneider, T. R., and Sheldrick, G. M. (2002) *Acta Crystallogr. Sect. D Biol. Crystallogr.* **58,** 1772–1779
27. Cowtan, K., and Main, P. (1998) *Acta Crystallogr. Sect. D Biol. Crystallogr.* **54,** 487–493
28. Perrakis, A., Morris, R., and Lamzin, V. S. (1999) *Nat. Struct. Biol.* **6,** 458–463
29. Jones, T. A., Zou, J. Y., Cowan, S. W., and Kjelgaard, M. (1991) *Acta Crystallogr. Sect. A* **47,** 110–119
30. Murshudov, G. N., Vagin, A. A., and Dodson, E. J. (1997) *Acta Crystallogr. Sect. D Biol. Crystallogr.* **53,** 240–255
31. Brunger, A. T. (1992) *Nature* **355,** 472–475
32. Laskowski, R. A., MacArthur, M. W., Moss, D. S., and Thornton, J. M. (1993) *J. Appl. Crystallogr.* **26,** 283–291
33. Altschul, S. F., Madden, T. L., Schäffer, A. A., Zhang, J., Zhang, Z., Miller, W., and Lipman, D. J. (1997) *Nucleic Acids Res.* **25,** 3389–3402
34. Thompson, J. D., Gibson, T. J., Plewniak, F., Jeanmougin, F., and Higgins, D. G. (1997) *Nucleic Acids Res.* **25,** 4876–4882
35. Sanner, M. F., Olson, A. J., and Spehner, J. C. (1996) *Biopolymers* **38,** 305–320
36. Holm, L., and Sander, C. (1993) *J. Mol. Biol.* **233,** 123–138
37. Wallace, A. C., Laskowski, R. A., and Thornton, J. M. (1995) *Protein Eng.* **8,** 127–134
38. Kraulis, P. J. (1991) *J. Appl. Crystallogr.* **24,** 946–950
39. Tamada, T., Kitadokoro, K., Higuchi, Y., Inaka, K., Yasui, A., de Ruiter, P. E., Eker, A. P., and Miki, K. (1997) *Nat. Struct. Biol.* **4,** 887–891
40. Merritt, E. A., and Bacon, D. J. (1997) *Methods Enzymol.* **277,** 505–524
41. Christendat, D., Yee, A., Dharamsi, A., Kluger, Y., Savchenko, A., Cort, J. R., Booth, V., Mackereth, C. D., Saridakis, V., Ekiel, I., Kozlov, G., Maxwell, K. L., Wu, N., McIntosh, L. P., Gehring, K., Kennedy, M. A., Davidson, A. R., Pai, E. F., Gerstein, M., Edwards, A. M., and Arrowsmith, C. H. (2000) *Nat. Struct. Biol.* **7,** 903–909
42. Liepinsh, E., Kitamura, M., Murakami, T., Nakaya, T., and Otting, G. (1997) *Nat. Struct. Biol.* **4,** 975–979
43. Murzin, A. G. (1998) *Nat. Struct. Biol.* **5,** 101
44. Karplus, P. A., Daniels, M. J., and Herriott, J. R. (1991) *Science* **251,** 60–66
45. Schroder, I., Johnson, E., and de Vries, S. (2003) *FEMS Microbiol. Rev.* **27,** 427–447
46. Heck, A. J. R., and van den Heuvel, R. H. H. (2004) *Mass Spectrom. Rev.*, in press
47. Loo, J. A. (1997) *Mass Spectrom. Rev.* **16,** 1–23
48. Fenn, J. B., Mann, M., Meng, C. K., Wong, S. F., and Whitehouse, C. M. (1989) *Science* **246,** 64–71
49. Tahallah, N., Van Den Heuvel, R. H. H., Van Den Berg, W. A., Maier, C. S., Van Berkel, W. J. H., and Heck, A. J. R. (2002) *J. Biol. Chem.* **277,** 36425–36432
50. Filisetti, L., Fontecave, M., and Nivière, V. (2003) *J. Biol. Chem.* **278,** 296–303
51. Chien, Y., and Weber, G. (1973) *Biochem. Biophys. Res. Commun.* **50,** 538–543
52. Bell, C. E., Yeates, T. O., and Eisenberg, D. (1997) *Protein Sci.* **6,** 2084–2096
53. Tanner, J. J., Tu, S. C., Barbour, L. J., Barnes, C. L., and Krause, K. L. (1999) *Protein Sci.* **8,** 1725–1732
54. Singh, S. K., Kurnasov, O. V., Chen, B., Robinson, H., Grishin, N. V., Osterman, A. L., and Zhang, H. (2002) *J. Biol. Chem.* **277,** 33291–33299
55. Smith, P. E., and Tanner, J. J. (2000) *J. Mol. Recognit.* **13,** 27–34
56. Park, H. W., Kim, S. T., Sancar, A., and Deisenhofer, J. (1995) *Science* **268,** 1866–1872

Structural Studies on Flavin Reductase PheA2 Reveal Binding of NAD in an Unusual Folded Conformation and Support Novel Mechanism of Action

Robert H. H. van den Heuvel, Adrie H. Westphal, Albert J. R. Heck, Martin A. Walsh, Stefano Rovida, Willem J. H. van Berkel and Andrea Mattevi

J. Biol. Chem. 2004, 279:12860-12867.
doi: 10.1074/jbc.M313765200 originally published online December 31, 2003
